Hybrid Precoder and Combiner Design with Low Resolution Phase Shifters in mmWave MIMO Systems

Zihuan Wang, *Student Member, IEEE,* Ming Li, *Senior Member, IEEE,* Qian Liu, *Member, IEEE,* and A. Lee Swindlehurst, *Fellow, IEEE*

arXiv:1710.06192v1 [cs.IT] 17 Oct 2017

***Abstract*—Millimeter wave (mmWave) communications have been considered as a key technology for next generation cellular systems and Wi-Fi networks because of its advances in providing orders-of-magnitude wider bandwidth than current wireless networks. Economical and energy-efficient analog/digial hybrid precoding and combining transceivers have been often proposed for mmWave massive multiple-input multiple-output (MIMO) systems to overcome the severe propagation loss of mmWave channels. One major shortcoming of existing solutions lies in the assumption of infinite or high-resolution phase shifters (PSs) to realize the analog beamformers. However, low-resolution PSs are typically adopted in practice to reduce the hardware cost and power consumption. Motivated by this fact, in this paper, we investigate the practical design of hybrid precoders and combiners with *low-resolution* PSs in mmWave MIMO systems. In particular, we propose an iterative algorithm which successively designs the low-resolution analog precoder and combiner pair for each data stream, aiming at conditionally maximizing the spectral efficiency. Then, the digital precoder and combiner are computed based on the obtained effective baseband channel to further enhance the spectral efficiency. In an effort to achieve an even more hardware-efficient large antenna array, we also investigate the design of hybrid beamformers with *one-bit* resolution (binary) PSs, and present a novel binary analog precoder and combiner optimization algorithm with quadratic complexity in the number of antennas. The proposed low-resolution hybrid beamforming design is further extended to multiuser MIMO communication systems. Simulation results demonstrate the performance advantages of the proposed algorithms compared to existing low-resolution hybrid beamforming designs, particularly for the one-bit resolution PS scenario.**

***Index Terms*—Millimeter wave (mmWave) communications, hybrid precoder, multiple-input multiple-output (MIMO), phase shifters, one-bit quantization.**

I. Introduction

The past decade has witnessed the exponential growth of data traffic along with the rapid proliferation of wireless devices. This flood of mobile traffic has significantly exacerbated spectrum congestion in current frequency bands, and therefore stimulated intensive interest in exploiting new spectrum bands for wireless communications. Millimeter wave (mmWave) wireless communications, operating in the frequency bands from 30-300 GHz, have been demonstrated as a promising candidate to fundamentally solve the spectrum congestion problem [1]-[3].

However, challenges always come along with opportunities. MmWave communications still need to overcome several technical difficulties before real-world deployment. As a negative result of the ten-fold increase of the carrier frequency, the propagation loss in mmWave bands is much higher than that of conventional frequency bands (e.g. 2.4 GHz) due to atmospheric absorption, rain attenuation, and low penetration [4]. From a positive perspective, the smaller wavelength of mmWave signals allows a large antenna array to be packed in a small physical dimension [5]. With the aid of pre/post-coding techniques in massive multiple-input multiple-output (MIMO) systems, the large antenna array can provide sufficient beamforming gain to overcome the severe propagation loss of mmWave channels. It also enables simultaneous transmission of multiple data streams resulting in significant improvements to spectral efficiency.

For MIMO systems operating in conventional cellular frequency bands, the full-digital precoder and combiner are completely realized in the digital domain by adjusting both the magnitude and phase of the baseband signals. However, these conventional full-digital schemes require a large number of expensive and energy-intensive radio frequency (RF) chains, analog-to-digital converters (ADCs), and digital-to-analog converters (DACs). Since mmWave communication systems operate at much higher carrier frequencies and wider bandwidths, the enormous cost and power consumption of the required RF chains and ADCs/DACs make the adoption of full-digital precoding and combining schemes impractical for mmWave systems. Recently, economical and energy-efficient analog/digital hybrid precoders and combiners have been advocated as a promising approach to tackle this issue. The hybrid precoding approaches adopt a large number of phase shifters (PSs) to implement high-dimensional analog precoders to compensate for the severe path-loss at mmWave bands, and a small number of RF chains and DACs to realize low-dimensional digital precoders to provide the necessary flexibility to perform advanced multiplexing/multiuser techniques.

Zihuan Wang and Ming Li are with the School of Information and Communication Engineering, Dalian University of Technology, Dalian, Liaoning 116024, China, (e-mail: wangzihuan@mail.dlut.edu.cn, mli@dlut.edu.cn).

Qian Liu is with the School of Computer Science and Technology, Dalian University of Technology, Dalian, Liaoning 116024, China (e-mail: qianliu@dlut.edu.cn).

A. L. Swindlehurst is with the Center for Pervasive Communications and Computing, University of California, Irvine, CA 92697 USA and also with the Institute for Advanced Study, Technical University of Munich,Munchen 80333, Germany (e-mail: swindle@uci.edu).

This paper is supported by the National Natural Science Foundation of China (Grant No. 61671101 and 61601080) and the Fundamental Research Funds for the Central Universities (Grant No. DUT15RC(3)121 and DUT17JC10).

The investigation of hybrid precoder and combiner design has attracted extensive attention in recent years because of its potential energy efficiency for mmWave MIMO communications. The major challenges in designing hybrid precoders are the practical constraints associated with the analog components, such as the requirement that the analog precoding be implemented with constant modulus PSs. Thus, hybrid precoder design typically requires the solution of various matrix factorization problems with constant modulus constraints. In particular, a popular solution to maximize the spectral efficiency of point-to-point transmission is to minimize the Euclidean distance between the hybrid precoder and the full-digital precoder [6]-[10]. Hybrid precoder design for partially-connected architectures are also studied in [11]-[13]. Due to the special characteristics of mmWave channels, codebook-based hybrid precoder designs are commonly proposed [14]-[18], in which the columns of the analog precoder are selected from certain candidate vectors, such as array response vectors of the channel and discrete Fourier transform (DFT) beamformers. Extensions of the hybrid beamformer design to multiuser mmWave MIMO systems have also been investigated in [19]-[27].

The aforementioned existing hybrid precoder and combiner designs generally assume that infinite or high-resolution PSs are used for implementing the analog beamformers in order to achieve satisfactory performance close to the full-digital scheme. However, implementing infinite/high-resolution PSs at mmWave frequencies would significantly increase the energy consumption and complexity of the required hardware circuits [28], [29]. Obviously, it is impractical to employ infinite/high-resolution PSs for mmWave systems and real-world analog beamformers will be implemented with low-resolution PSs. Consequently, an important research direction is the exploration of signal processing techniques for hybrid analog/digital architectures that can mitigate the loss of beamforming accuracy due to the low-resolution PSs.

A straightforward approach to obtain the finite-resolution beamformer is to design the infinite-resolution analog beamformer first, and then directly quantize each phase term to a finite set [30]. However, this solution becomes inefficient when the PSs have very low resolution. An alternative solution for hybrid beamforming with finite-resolution PSs is codebook-based design [14]-[18]. However, for low-resolution PSs, the size of the codebook is very small and the resulting performance is not satisfactory. In [31], [32], Sohrabi and Yu proposed to iteratively design the low-resolution hybrid precoder to maximize the spectral efficiency. However, the performance of this algorithm often suffers when one-bit quantized PSs are applied.

In this paper, we first consider the problem of designing hybrid precoders and combiners with low-resolution PSs for a point-to-point mmWave MIMO system. The objective of the proposed algorithm is to minimize the performance loss caused by the low-resolution PSs while maintaining a low computational complexity. To achieve this goal, we propose to successively design the low-resolution analog precoder and combiner pair for each data stream, aiming at conditionally maximizing the spectral efficiency. An iterative phase matching algorithm is introduced to implement the low-resolution analog precoder and combiner pair. Then, the digital precoder and combiner are computed based on the obtained effective baseband channel to further enhance the spectral efficiency.

Note that the power consumption and cost of the PS are proportional to its resolution. For example, a 4-bit (i.e. 22.5°) resolution PS at mmWave frequencies requires 45-106 mW, while a 3-bit (i.e. 45°) resolution PS needs only 15 mW [29]. In an effort to achieve maximum hardware efficiency, we also investigate the design of hybrid beamformers with one-bit resolution (binary) PSs. Inspired by the findings in [33], we present a binary analog precoder and combiner optimization algorithm under a rank-1 approximation of the interference-included equivalent channel. This algorithm has quadratic complexity in the number of antennas and can achieve almost the same performance as the optimal exhaustive search method. Finally, our investigation of low-resolution hybrid precoders and combiners is extended to multiuser mmWave MIMO systems. Numerical results in the simulation section demonstrate that the proposed algorithms can offer a performance improvement compared with existing low-resolution hybrid beamforming schemes, especially for the one-bit resolution PS scenario.

Notation: The following notation is used throughout this paper. Boldface lower-case and upper-case letters indicate column vectors and matrices, respectively. $(\cdot)^T$ and $(\cdot)^H$ denote the transpose and transpose-conjugate operations, respectively. $\mathbb{E}\{\cdot\}$ represents statistical expectation. $\mathfrak{Re}\{\cdot\}$ extracts the real part of a complex number; $\mathrm{sign}(\cdot)$ denotes the sign operator; $\mathrm{angle}\{\cdot\}$ represents the phase of a complex number. $\mathbf{I}_L$ indicates an $L \times L$ identity matrix. $\mathbb{C}$ denotes the set of complex numbers. $|\mathbf{A}|$ denotes the determinant of matrix $\mathbf{A}$. $|\mathcal{A}|$ denotes the cardinality of set $\mathcal{A}$. $|a|$ and $\|\mathbf{a}\|$ are the magnitude and norm of a scalar a and vector $\mathbf{a}$, respectively. $\|\mathbf{A}\|_F$ denotes the Frobenius norm of matrix $\mathbf{A}$. Finally, we adopt a Matlab-like matrix indexing notation: $\mathbf{A}(:,i)$ denotes the i-th column of matrix $\mathbf{A}$; $\mathbf{A}(i,j)$ denotes the element of the i-th row and the j-th column of matrix $\mathbf{A}$; $\mathbf{a}(i)$ denotes the i-th element of vector $\mathbf{a}$.

II. System Model and Problem Formulation

A. Point-to-Point mmWave MIMO System Model

We first consider a point-to-point mmWave MIMO system using a hybrid precoder and combiner with low-resolution PSs, as illustrated in Fig. 1. The transmitter employs N_t antennas and N_t^{RF} RF chains to simultaneously transmit N_s data streams to the receiver which is equipped with N_r antennas and N_r^{RF} RF chains. To ensure the efficiency of the mmWave communication with a limited number of RF chains, the number of data streams and the number of RF chains are constrained as $N_s = N_t^{RF} = N_r^{RF}$.

The transmitted symbols are first processed by a baseband digital precoder $\mathbf{F}_{BB} \in \mathbb{C}^{N_t^{RF} \times N_s}$, then up-converted to the RF domain via N_t^{RF} RF chains before being precoded with an analog precoder $\mathbf{F}_{RF}$ of dimension $N_t \times N_t^{RF}$. While the baseband digital precoder $\mathbf{F}_{BB}$ enables both amplitude and phase modifications, the elements of the analog precoder

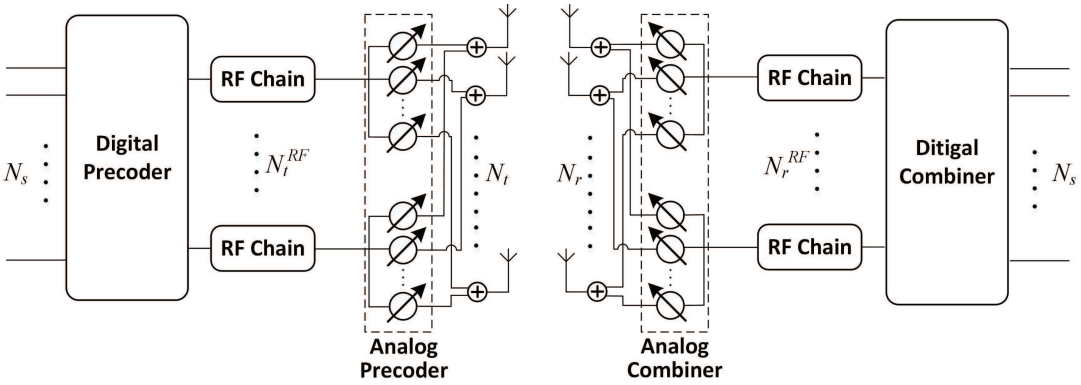


Fig. 1. The point-to-point mmWave MIMO system using hybrid precoder and combiner.

$\mathbf{F}_{RF}$, which are implemented by the PSs, have a constant amplitude $\frac{1}{\sqrt{N_t}}$ and quantized phases: $\mathbf{F}_{RF}(i,j) = \frac{1}{\sqrt{N_t}} e^{j\vartheta_{i,j}}$, in which the phase $\vartheta_{i,j}$ is quantized as $\vartheta_{i,j} \in \mathcal{B} \triangleq \{\frac{2\pi b}{2^B} \mid b = 1, 2, \ldots, 2^B\}$, and B is the number of bits to control the phase. We denote the constraint set of the analog precoder as follows: $\mathbf{F}_{RF}(i,j) \in \mathcal{F} \triangleq \{\frac{1}{\sqrt{N_t}} e^{j\frac{2\pi b}{2^B}} \mid b = 1, 2, \ldots, 2^B\}$. Obviously, a larger number of bits B leads to finer resolution for the PSs and potentially better performance, but also results in higher hardware complexity and power consumption.

The discrete-time transmitted signal can be written in the following form

$$\mathbf{x} = \sqrt{P}\mathbf{F}_{RF}\mathbf{F}_{BB}\mathbf{s} \tag{1}$$

where $\mathbf{s}$ is the $N_s \times 1$ symbol vector, $\mathbb{E}\{\mathbf{s}\mathbf{s}^H\} = \frac{1}{N_s}\mathbf{I}_{N_s}$, P represents transmit power and this power constraint is enforced by normalizing $\mathbf{F}_{BB}$ such that $\|\mathbf{F}_{RF}\mathbf{F}_{BB}\|_F^2 = N_s$.

We consider a narrow-band slow-fading propagation channel, which yields the following received signal

$$\begin{aligned} \mathbf{y} &= \mathbf{H}\mathbf{x} + \mathbf{n} \\ &= \sqrt{P}\mathbf{H}\mathbf{F}_{RF}\mathbf{F}_{BB}\mathbf{s} + \mathbf{n} \end{aligned} \tag{2}$$

where $\mathbf{y}$ is the $N_r \times 1$ received signal vector, $\mathbf{H}$ is the $N_r \times N_t$ channel matrix, and $\mathbf{n} \sim \mathcal{CN}(\mathbf{0}, \sigma^2\mathbf{I}_{N_r})$ is the complex Gaussian noise vector corrupting the received signal.

The receiver employs an analog combiner implemented by the PSs and a digital combiner using N_r^{RF} RF chains to process the received signal. The signal after the spatial processing has the form

$$\widehat{\mathbf{s}} = \sqrt{P}\mathbf{W}_{BB}^H\mathbf{W}_{RF}^H\mathbf{H}\mathbf{F}_{RF}\mathbf{F}_{BB}\mathbf{s} + \mathbf{W}_{BB}^H\mathbf{W}_{RF}^H\mathbf{n} \tag{3}$$

where $\mathbf{W}_{RF}$ is the $N_r \times N_r^{RF}$ analog combiner whose elements have the same constraint as $\mathbf{F}_{RF}$, i.e. $\mathbf{W}_{RF}(i,j) = \frac{1}{\sqrt{N_r}} e^{j\varphi_{i,j}}$, $\varphi_{i,j} \in \mathcal{B}$ and thus $\mathbf{W}_{RF}(i,j) \in \mathcal{W} \triangleq \{\frac{1}{\sqrt{N_r}} e^{j\frac{2\pi b}{2^B}} \mid b = 1, 2, \ldots, 2^B\}$, $\mathbf{W}_{BB}$ is the $N_r^{RF} \times N_s$ digital baseband combiner and the combiner matrices are normalized such that $\|\mathbf{W}_{RF}\mathbf{W}_{BB}\|_F^2 = N_s$.

B. Problem Formulation

We consider the practical and hardware-efficient scenario in which the PSs have very low-resolution (e.g. $B = 1, 2$) to reduce the power consumption and complexity. Under this hardware constraint, we aim to jointly design the hybrid precoder and combiner for a mmWave MIMO system. When Gaussian symbols are transmitted over the mmWave MIMO channel, the achievable spectral efficiency is given by

$$R = \log_2\left(\left|\mathbf{I}_{N_s} + \frac{P}{N_s}\mathbf{R}_n^{-1}\mathbf{W}_{BB}^H\mathbf{W}_{RF}^H\mathbf{H}\mathbf{F}_{RF}\mathbf{F}_{BB} \times \mathbf{F}_{BB}^H\mathbf{F}_{RF}^H\mathbf{H}^H\mathbf{W}_{RF}\mathbf{W}_{BB}\right|\right), \tag{4}$$

where $\mathbf{R}_n \triangleq \sigma_n^2\mathbf{W}_{BB}^H\mathbf{W}_{RF}^H\mathbf{W}_{RF}\mathbf{W}_{BB}$ is the noise covariance matrix after combining. We aim to jointly design the digital beamformers $\mathbf{F}_{BB}$, $\mathbf{W}_{BB}$ as well as the low-resolution analog beamformers $\mathbf{F}_{RF}$, $\mathbf{W}_{RF}$ to maximize the spectral efficiency:

$$\begin{aligned} \left\{\mathbf{F}_{RF}^\star, \mathbf{F}_{BB}^\star, \mathbf{W}_{RF}^\star, \mathbf{W}_{BB}^\star\right\} = \arg\max\ & R \\ \text{s. t.} \quad & \mathbf{F}_{RF}(i,j) \in \mathcal{F}, \forall i,j, \\ & \mathbf{W}_{RF}(i,j) \in \mathcal{W}, \forall i,j, \\ & \|\mathbf{F}_{RF}\mathbf{F}_{BB}\|_F^2 = N_s, \\ & \|\mathbf{W}_{RF}\mathbf{W}_{BB}\|_F^2 = N_s. \end{aligned} \tag{5}$$

Obviously, the optimization problem (5) is a non-convex NP-hard problem. In the next section, we attempt to decompose the original problem into a series of sub-problems and seek a sub-optimal solution with low-complexity and satisfactory performance.

III. Low-Resolution Hybrid Precoder and Combiner Design

To simplify the joint hybrid precoder and combiner design, the objective problem is decomposed into two separate optimizations. We first focus on the joint design of the analog precoder $\mathbf{F}_{RF}$ and combiner $\mathbf{W}_{RF}$. Then, having the effective baseband channel associated with the obtained optimal analog precoder and combiner, the digital precoder $\mathbf{F}_{BB}$ and combiner $\mathbf{W}_{BB}$ are computed to further maximize the spectral efficiency.

A. Low-Resolution Analog Precoder and Combiner Design

We observe that under the assumption of high signal-to-noise-ratio (SNR), the achievable spectral efficiency in (4) can be approximated as

$$R \approx \log_2\left(\left|\frac{P}{N_s}\mathbf{R}_n^{-1}\mathbf{W}_{BB}^H\mathbf{W}_{RF}^H\mathbf{H}\mathbf{F}_{RF}\mathbf{F}_{BB}\times \mathbf{F}_{BB}^H\mathbf{F}_{RF}^H\mathbf{H}^H\mathbf{W}_{RF}\mathbf{W}_{BB}\right|\right). \quad (6)$$

While the per-antenna SNR in mmWave systems is typically low, the post-combining SNR should be high enough to justify this approximation. In addition, it has been verified in [32] that for large-scale MIMO systems, the optimal analog beamformers are approximately orthogonal, i.e. $\mathbf{F}_{RF}^H\mathbf{F}_{RF} \propto \mathbf{I}_{N_t^{RF}}$. This enables us to assume $\mathbf{F}_{BB}\mathbf{F}_{BB}^H \approx \zeta^2\mathbf{I}_{N_s}$ when $N_t^{RF} = N_s$, where ζ^2 is a normalization factor. Similarly, we have $\mathbf{W}_{BB}\mathbf{W}_{BB}^H \approx \xi^2\mathbf{I}_{N_s}$ and $\mathbf{W}_{BB}^H\mathbf{W}_{RF}^H\mathbf{W}_{RF}\mathbf{W}_{BB} \approx \mathbf{I}_{N_s}$. Let $\gamma^2 \triangleq \zeta^2\xi^2$, then (6) can be further simplified as

$$R \approx \log_2\left(\left|\frac{P\gamma^2}{N_s\sigma^2}\mathbf{W}_{RF}^H\mathbf{H}\mathbf{F}_{RF}\mathbf{F}_{RF}^H\mathbf{H}^H\mathbf{W}_{RF}\right|\right) \quad (7)$$

$$\overset{(a)}{=} N_s\log_2\left(\frac{P\gamma^2}{N_s\sigma^2}\right) + 2\times\log_2\left(\left|\mathbf{W}_{RF}^H\mathbf{H}\mathbf{F}_{RF}\right|\right) \quad (8)$$

where (a) follows since $|\mathbf{X}\mathbf{Y}| = |\mathbf{X}||\mathbf{Y}|$ when $\mathbf{X}$ and $\mathbf{Y}$ are both square matrices. Therefore, the analog precoder and combiner design with low-resolution PSs can be approximately reformulated as:

$$\begin{aligned}\{\mathbf{F}_{RF}^\star, \mathbf{W}_{RF}^\star\} = \arg\max\ & \log_2\left(\left|\mathbf{W}_{RF}^H\mathbf{H}\mathbf{F}_{RF}\right|\right)\\ \text{s.t. } & \mathbf{F}_{RF}(i,j) \in \mathcal{F}, \forall i,j,\\ & \mathbf{W}_{RF}(i,j) \in \mathcal{W}, \forall i,j.\end{aligned} \quad (9)$$

Unfortunately, the optimization problem (9) is still NP-hard and has exponential complexity $\mathcal{O}(|\mathcal{F}|^{N_tN_t^{RF}}|\mathcal{W}|^{N_rN_r^{RF}})$. Therefore, we propose to further decompose this difficult optimization problem into a series of sub-problems, in which each transmit/receive RF chain pair is considered one by one and the analog precoder and combiner for each pair are successively designed.

In particular, we define the singular value decomposition (SVD) of $\mathbf{H}$ as

$$\mathbf{H} = \mathbf{U}\mathbf{\Sigma}\mathbf{V}^H \quad (10)$$

where $\mathbf{U}$ is an $N_r\times N_r$ unitary matrix, $\mathbf{V}$ is an $N_t\times N_t$ unitary matrix, and $\mathbf{\Sigma}$ is a rectangular diagonal matrix of singular values. Due to the sparse nature of the mmWave channel, the matrix $\mathbf{H}$ is typically low rank. In particular, the effective rank of the channel serves as an upper bound for the number of data streams N_s that the channel can support. Thus, we assume that the channel $\mathbf{H}$ can be well approximated by retaining only the N_s strongest components $\mathbf{H} \approx \widehat{\mathbf{U}}\widehat{\mathbf{\Sigma}}\widehat{\mathbf{V}}^H$, where $\widehat{\mathbf{U}} \triangleq \mathbf{U}(:, 1:N_s)$, $\widehat{\mathbf{\Sigma}} \triangleq \mathbf{\Sigma}(1:N_s, 1:N_s)$, and $\widehat{\mathbf{V}} \triangleq \mathbf{V}(:, 1:N_s)$. Then, the objective in (9) can be converted to

$$\log_2\left(\left|\mathbf{W}_{RF}^H\mathbf{H}\mathbf{F}_{RF}\right|\right) \approx \log_2\left(\left|\mathbf{W}_{RF}^H\widehat{\mathbf{U}}\widehat{\mathbf{\Sigma}}\widehat{\mathbf{V}}^H\mathbf{F}_{RF}\right|\right). \quad (11)$$

Next, we write the analog precoding and combining matrices as $\mathbf{F}_{RF} \triangleq [\mathbf{f}_{RF,1}\dots\mathbf{f}_{RF,N_s}]$ and $\mathbf{W}_{RF} \triangleq [\mathbf{w}_{RF,1}\dots\mathbf{w}_{RF,N_s}]$, respectively, where $\mathbf{f}_{RF,l}$ and $\mathbf{w}_{RF,l}$, $l = 1,\dots,N_s$, are the analog precoder and combiner pair for the l-th data stream. Furthermore, we denote $\mathbf{F}_{RF,\backslash l}$ as the precoding matrix excluding the l-th precoder vector $\mathbf{f}_{RF,l}$ and $\mathbf{W}_{RF,\backslash l}$ as the combining matrix excluding the l-th combiner vector $\mathbf{w}_{RF,l}$. Then, the formulation (11) can be further transformed to (12)-(16), which are presented at the top of following page, where α is a very small scalar to assure invertibility. Thus, the objective in (9) can be reformulated as:

$$\log_2\left(\left|\mathbf{W}_{RF}^H\mathbf{H}\mathbf{F}_{RF}\right|\right) \approx \log_2\left(\left|\mathbf{W}_{RF,\backslash l}^H\mathbf{H}\mathbf{F}_{RF,\backslash l}\right|\right) + \log_2\left(\left|\mathbf{w}_{RF,l}^H\mathbf{Q}_l\mathbf{f}_{RF,l}\right|\right) \quad (17)$$

where we define the interference-included channel matrix $\mathbf{Q}_l$ as

$$\mathbf{Q}_l \triangleq \widehat{\mathbf{U}}(\alpha\mathbf{I}_{N_s} + \widehat{\mathbf{\Sigma}}\widehat{\mathbf{V}}^H\mathbf{F}_{RF,\backslash l}\mathbf{W}_{RF,\backslash l}^H\widehat{\mathbf{U}})^{-1}\widehat{\mathbf{\Sigma}}\widehat{\mathbf{V}}^H. \quad (18)$$

According to (17), if $\mathbf{F}_{RF,\backslash l}$ and $\mathbf{W}_{RF,\backslash l}$ are known, the problem (9) can be reformulated as finding a corresponding precoder $\mathbf{f}_{RF,l}$ and combiner $\mathbf{w}_{RF,l}$ pair to conditionally maximize the achievable spectral efficiency:

$$\begin{aligned}\{\mathbf{f}_{RF,l}^\star, \mathbf{w}_{RF,l}^\star\} = \arg\max\ & \left|\mathbf{w}_{RF,l}^H\mathbf{Q}_l\mathbf{f}_{RF,l}\right|\\ \text{s.t. } & \mathbf{f}_{RF,l}(i) \in \mathcal{F},\ i = 1,\dots,N_t,\\ & \mathbf{w}_{RF,l}(j) \in \mathcal{W},\ j = 1,\dots,N_r.\end{aligned} \quad (19)$$

This motivates us to propose an iterative algorithm, which starts with appropriate initial RF precoding and combining matrices then successively designs $\mathbf{f}_{RF,l}$ and $\mathbf{w}_{RF,l}$ according to (19) with an updated $\mathbf{Q}_l$ as in (18) until the algorithm converges.

The complexity of obtaining an optimal solution to (19) for each iteration is now reduced to $\mathcal{O}(|\mathcal{F}|^{N_t}|\mathcal{W}|^{N_r})$, which is still too high. To practically solve the problem (19), in what follows we present an iterative phase matching algorithm, which searches the conditionally optimal phase of each element of the analog precoder $\mathbf{f}_{RF,l}$ and combiner $\mathbf{w}_{RF,l}$. Specifically, we first design the analog precoder $\mathbf{f}_{RF,l}$ assuming the analog combiner $\mathbf{w}_{RF,l}$ is fixed. Let $\vartheta_{l,i}$ be the phase of the i-th element of the analog precoder $\mathbf{f}_{RF,l}$ and let $\varphi_{l,j}$ be the phase of the j-th element of the analog combiner $\mathbf{w}_{RF,l}$. If we temporarily remove the discrete phase constraint, the optimal continuous phase $\tilde{\vartheta}_{l,i}$ of the i-th element of the analog precoder $\mathbf{f}_{RF,l}$ is given by the following proposition, whose proof is provided in Appendix A.

Proposition 1: Given the phases $\varphi_{l,j}$ of the analog combiner $\mathbf{w}_{RF,l}$ and the phases $\vartheta_{l,u}$, $u \neq i$, of the analog precoder $\mathbf{f}_{RF,l}$, the optimal continuous phase $\tilde{\vartheta}_{l,i}$ of the i-th element of analog

$$\log_2\left(\left|\mathbf{W}_{RF}^H\widehat{\mathbf{U}}\widehat{\mathbf{\Sigma}}\widehat{\mathbf{V}}^H\mathbf{F}_{RF}\right|\right)=\log_2\left(\left|\widehat{\mathbf{\Sigma}}\widehat{\mathbf{V}}^H\mathbf{F}_{RF}\mathbf{W}_{RF}^H\widehat{\mathbf{U}}\right|\right) \tag{12}$$

$$=\log_2\left(\left|\widehat{\mathbf{\Sigma}}\widehat{\mathbf{V}}^H\left[\mathbf{F}_{RF,\backslash l}\ \mathbf{f}_{RF,l}\right]\left[\mathbf{W}_{RF,\backslash l}\ \mathbf{w}_{RF,l}\right]^H\widehat{\mathbf{U}}\right|\right)=\log_2\left(\left|\widehat{\mathbf{\Sigma}}\widehat{\mathbf{V}}^H\mathbf{F}_{RF,\backslash l}\mathbf{W}_{RF,\backslash l}^H\widehat{\mathbf{U}}+\widehat{\mathbf{\Sigma}}\widehat{\mathbf{V}}^H\mathbf{f}_{RF,l}\mathbf{w}_{RF,l}^H\widehat{\mathbf{U}}\right|\right) \tag{13}$$

$$\approx\log_2\left(\left|\left(\widehat{\mathbf{\Sigma}}\widehat{\mathbf{V}}^H\mathbf{F}_{RF,\backslash l}\mathbf{W}_{RF,\backslash l}^H\widehat{\mathbf{U}}\right)\left[\mathbf{I}_{N_s}+\left(\alpha\mathbf{I}_{N_s}+\widehat{\mathbf{\Sigma}}\widehat{\mathbf{V}}^H\mathbf{F}_{RF,\backslash l}\mathbf{W}_{RF,\backslash l}^H\widehat{\mathbf{U}}\right)^{-1}\widehat{\mathbf{\Sigma}}\widehat{\mathbf{V}}^H\mathbf{f}_{RF,l}\mathbf{w}_{RF,l}^H\widehat{\mathbf{U}}\right]\right|\right) \tag{14}$$

$$=\log_2\left(\left|\widehat{\mathbf{\Sigma}}\widehat{\mathbf{V}}^H\mathbf{F}_{RF,\backslash l}\mathbf{W}_{RF,\backslash l}^H\widehat{\mathbf{U}}\right|\right)+\log_2\left(\left|\left[\mathbf{I}_{N_s}+\left(\alpha\mathbf{I}_{N_s}+\widehat{\mathbf{\Sigma}}\widehat{\mathbf{V}}^H\mathbf{F}_{RF,\backslash l}\mathbf{W}_{RF,\backslash l}^H\widehat{\mathbf{U}}\right)^{-1}\widehat{\mathbf{\Sigma}}\widehat{\mathbf{V}}^H\mathbf{f}_{RF,l}\mathbf{w}_{RF,l}^H\widehat{\mathbf{U}}\right]\right|\right) \tag{15}$$

$$=\log_2\left(\left|\mathbf{W}_{RF,\backslash l}^H\widehat{\mathbf{U}}\widehat{\mathbf{\Sigma}}\widehat{\mathbf{V}}^H\mathbf{F}_{RF,\backslash l}\right|\right)+\log_2\left(\left|\left[1+\mathbf{w}_{RF,l}^H\widehat{\mathbf{U}}\left(\alpha\mathbf{I}_{N_s}+\widehat{\mathbf{\Sigma}}\widehat{\mathbf{V}}^H\mathbf{F}_{RF,\backslash l}\mathbf{W}_{RF,\backslash l}^H\widehat{\mathbf{U}}\right)^{-1}\widehat{\mathbf{\Sigma}}\widehat{\mathbf{V}}^H\mathbf{f}_{RF,l}\right]\right|\right) \tag{16}$$

precoder $\mathbf{f}_{RF,l}$ is

$$\tilde{\vartheta}_{l,i}=\text{angle}\left\{\sum_{j=1}^{N_r}e^{j\varphi_{l,j}}\sum_{u\neq i}^{N_t}e^{j\vartheta_{l,u}}\mathbf{Q}_l(j,u)\right\}-\text{angle}\left\{\sum_{j=1}^{N_r}e^{j\varphi_{l,j}}\mathbf{Q}_l(j,i)\right\}. \tag{20}$$

■

Then, after finding the optimal continuous phase $\tilde{\vartheta}_{l,i}$ by (20), we reconsider the discrete phase constraint and find the optimal low-resolution phase $\vartheta_{l,i}$ by quantization:

$$\vartheta_{l,i}=\arg\min_{\hat{\vartheta}_{l,i}\in\mathcal{B}}\left|\tilde{\vartheta}_{l,i}-\hat{\vartheta}_{l,i}\right|. \tag{21}$$

Similarly, if the analog precoder $\mathbf{f}_{RF,l}$ is determined, the optimal continuous phase $\tilde{\varphi}_{l,j}$ of the j-th element of $\mathbf{w}_{RF,l}$ is

$$\tilde{\varphi}_{l,j}=\text{angle}\left\{\sum_{i=1}^{N_t}e^{j\vartheta_{l,i}}\sum_{u\neq j}^{N_t}e^{j\varphi_{l,u}}\mathbf{Q}_l(u,i)\right\}-\text{angle}\left\{\sum_{i=1}^{N_t}e^{j\varphi_{l,i}}\mathbf{Q}_l(j,i)\right\}, \tag{22}$$

and the optimal low-resolution phase $\varphi_{l,j}$ is obtained by

$$\varphi_{l,j}=\arg\min_{\hat{\varphi}_{l,j}\in\mathcal{B}}\left|\tilde{\varphi}_{l,j}-\hat{\varphi}_{l,j}\right|. \tag{23}$$

Motivated by (20)-(23), the iterative procedure to design the precoder $\mathbf{f}_{RF,l}$ and combiner $\mathbf{w}_{RF,l}$ as in (19) is straightforward. With appropriate initial $\vartheta_{l,i}$, $\varphi_{l,j}$, we design the precoder $\mathbf{f}_{RF,l}$ by finding the conditionally optimal phases $\vartheta_{l,i}$ as in (20) and (21). Then, with the obtained $\vartheta_{l,i}$, $i=1,\ldots,N_t$, we design the combiner $\mathbf{w}_{RF,l}$ by finding the conditionally optimal phases $\varphi_{l,j}$ as in (22) and (23). We alternate the designs of $\mathbf{f}_{RF,l}$ and $\mathbf{w}_{RF,l}$ iteratively until the obtained phase of each element of $\mathbf{f}_{RF,l}$ and $\mathbf{w}_{RF,l}$ does not change and the convergence is achieved. Note that since in each precoder and combiner design step, the objective function of (19) is monotonically non-decreasing, and thus our proposed algorithm is guaranteed to converge to at least a locally optimal solution.

We summarize the proposed joint low-resolution analog precoder and combiner design in Algorithm 1.

Algorithm 1 Iterative Phase Matching Algorithm for Low-Resolution Analog Precoder and Combiner Design

Input: $\mathcal{F}$, $\mathcal{W}$, $\mathbf{H}$.
Output: $\mathbf{F}_{RF}^\star$ and $\mathbf{W}_{RF}^\star$.

```
Initialize F*_RF = 0, W*_RF = 0.
for l = 1 : N_s do
    Obtain F_{RF,\l} from F*_RF and W_{RF,\l} from W*_RF.
    Update Q_l = Û(αI_{N_s} + Σ̂V̂^H F_{RF,\l} W^H_{RF,\l} Û)^{-1} Σ̂V̂^H.
    while no convergence of ϑ_{l,i} and φ_{l,j} do
        for i = 1 : N_t do
            Obtain quantized phase ϑ_{l,i} by (20) and (21).
        end for
        for j = 1 : N_r do
            Obtain quantized phase φ_{l,j} by (22) and (23).
        end for
    end while
    Construct f*_{RF,l} by ϑ_{l,i} and w*_{RF,l} by φ_{l,j}.
end for
Construct F*_RF by f*_{RF,l} and W*_RF by w*_{RF,l}.
Goto Step 2 until convergence of F*_RF and W*_RF.
```

B. Digital Precoder and Combiner Design

After all analog precoder-combiner pairs have been determined, we can obtain the effective baseband channel $\widetilde{\mathbf{H}}$ as

$$\widetilde{\mathbf{H}}\triangleq\left(\mathbf{W}_{RF}^\star\right)^H\mathbf{H}\mathbf{F}_{RF}^\star, \tag{24}$$

where $\mathbf{F}_{RF}^\star\triangleq[\mathbf{f}_{RF,1}^\star,\ldots,\mathbf{f}_{RF,N_s}^\star]$ and $\mathbf{W}_{RF}^\star\triangleq[\mathbf{w}_{RF,1}^\star,\ldots,\mathbf{w}_{RF,N_s}^\star]$. For the baseband precoder and combiner design, we define the SVD of the effective baseband channel $\widetilde{\mathbf{H}}$ as

$$\widetilde{\mathbf{H}}=\widetilde{\mathbf{U}}\widetilde{\mathbf{\Sigma}}\widetilde{\mathbf{V}}^H \tag{25}$$

where $\widetilde{\mathbf{U}}$ and $\widetilde{\mathbf{V}}$ are $N_s\times N_s$ unitary matrices, $\widetilde{\mathbf{\Sigma}}$ is an $N_s\times N_s$ diagonal matrix of singular values. Then, to further enhance the spectral efficiency, an SVD-based baseband digital precoder and combiner are employed:

$$\mathbf{F}_{BB}^\star=\widetilde{\mathbf{V}}, \tag{26}$$

$$\mathbf{W}_{BB}^\star=\widetilde{\mathbf{U}}. \tag{27}$$

Finally, the baseband precoder and combiner are normalized

$$\mathbf{F}_{BB}^{\star} = \frac{\sqrt{N_s}\mathbf{F}_{BB}^{\star}}{\|\mathbf{F}_{RF}^{\star}\mathbf{F}_{BB}^{\star}\|_F}, \tag{28}$$

$$\mathbf{W}_{BB}^{\star} = \frac{\sqrt{N_s}\mathbf{W}_{BB}^{\star}}{\|\mathbf{W}_{RF}^{\star}\mathbf{W}_{BB}^{\star}\|_F}. \tag{29}$$

IV. One-Bit Resolution Analog Precoder and Combiner Design

In the previous section, we proposed a novel hybrid beamformer design for maximizing the spectral efficiency of a mmWave MIMO system, in which the analog precoder and combiner are implemented with low-resolution PSs. In order to achieve maximum hardware efficiency, in this section we focus on the design of analog precoders and combiners using "one-bit" resolution (binary) PSs, which can maximally reduce the power consumption and simplify the hardware complexity. Although the iterative phase matching algorithm proposed in the previous section can also be applied, a simpler approach is possible in the one-bit case. Therefore, in this section, we present an efficient one-bit resolution analog beamformer design, which can achieve good performance with much lower complexity.

We follow the procedure of the hybrid beamforming design proposed in the previous section, but only modify the optimization problem (19), which attempts to determine the l-th analog precoder and combiner pair. Particularly, we reformulate this analog beamformer design problem (19) with the constraint of one-bit resolution PSs as

$$\left\{\mathbf{f}_{RF,l}^{\star}, \mathbf{w}_{RF,l}^{\star}\right\} = \arg \max_{\substack{\mathbf{f}_{RF,l}\in\frac{1}{\sqrt{N_t}}\{\pm 1\}^{N_t} \\ \mathbf{w}_{RF,l}\in\frac{1}{\sqrt{N_r}}\{\pm 1\}^{N_r}}} \left|\mathbf{w}_{RF,l}^H \mathbf{Q}_l \mathbf{f}_{RF,l}\right|. \tag{30}$$

The optimization problem (30) can be solved through exhaustive search with exponential complexity $\mathcal{O}(2^{N_t N_r})$, which would not be possible with large antenna arrays. Therefore, in the following we attempt to develop an efficient one-bit resolution beamformer design with polynomial complexity in the number of antennas.

We first define the SVD of $\mathbf{Q}_l$ as

$$\mathbf{Q}_l = \sum_{i=1}^{N_s} \lambda_{l,i}\mathbf{p}_{l,i}\mathbf{g}_{l,i}^H, \tag{31}$$

where $\mathbf{p}_{l,i}$ and $\mathbf{g}_{l,i}$ are the i-th left and right singular vectors of $\mathbf{Q}_l$, respectively, and $\lambda_{l,i}$ is the i-th largest singular value, $\lambda_{l,1} \geq \lambda_{l,2} \geq \ldots \geq \lambda_{l,N_s}$. Then, the objective in (30) can be rewritten as

$$|\mathbf{w}_{RF,l}^H \mathbf{Q}_l \mathbf{f}_{RF,l}| = \left|\sum_{i=1}^{N_s} \lambda_{l,i}\mathbf{w}_{RF,l}^H \mathbf{p}_{l,i}\mathbf{g}_{l,i}^H \mathbf{f}_{RF,l}\right|. \tag{32}$$

If we utilize a rank-1 approximation by keeping only the strongest term, i.e. $\mathbf{Q}_l \approx \lambda_{l,1}\mathbf{p}_{l,1}\mathbf{g}_{l,1}^H$, the optimization function in (30) can be approximated by

$$\left\{\mathbf{f}_{RF,l}^{\star}, \mathbf{w}_{RF,l}^{\star}\right\} = \arg \max_{\substack{\mathbf{f}_{RF,l}\in\frac{1}{\sqrt{N_t}}\{\pm 1\}^{N_t} \\ \mathbf{w}_{RF,l}\in\frac{1}{\sqrt{N_r}}\{\pm 1\}^{N_r}}} \left|\mathbf{w}_{RF,l}^H \mathbf{p}_{l,1}\mathbf{g}_{l,1}^H \mathbf{f}_{RF,l}\right|. \tag{33}$$

Now, the joint optimization problem (33) can be decoupled into individually designing the analog precoder $\mathbf{f}_{RF,l}$ and combiner $\mathbf{w}_{RF,l}$:

$$\mathbf{f}_{RF,l}^{\star} = \arg \max_{\mathbf{f}_{RF,l}\in\frac{1}{\sqrt{N_t}}\{\pm 1\}^{N_t}} \left|\mathbf{f}_{RF,l}^H \mathbf{g}_{l,1}\right|, \tag{34}$$

$$\mathbf{w}_{RF,l}^{\star} = \arg \max_{\mathbf{w}_{RF,l}\in\frac{1}{\sqrt{N_r}}\{\pm 1\}^{N_r}} \left|\mathbf{w}_{RF,l}^H \mathbf{p}_{l,1}\right|. \tag{35}$$

These two optimization problems (34) and (35) require only the singular vectors $\mathbf{p}_{l,1}$ and $\mathbf{g}_{l,1}$ associated with the largest singular value, which can be quickly obtained by the power iteration algorithm [34] instead of the complete SVD calculation. However, solving (34) and (35) by exhaustive search still has exponential complexity in the number of antennas. In order to further reduce the complexity without a significant loss of performance, we propose to construct a smaller dimension candidate beamformer set, from which the optimal beamformer can be found with linear complexity. In the following, we present this algorithm for the precoder design (34) as an example, while the combiner design (35) follows the same procedure.

We introduce an auxiliary variable $\phi \in [-\pi, \pi)$ and we reformulate the optimization problem (34) as:

$$\left\{\phi^{\star}, \mathbf{f}_{RF,l}^{\star}\right\} = \arg \max_{\substack{\phi\in[-\pi,\pi) \\ \mathbf{f}_{RF,l}\in\frac{1}{\sqrt{N_t}}\{\pm 1\}^{N_t}}} \mathfrak{Re}\left\{\mathbf{f}_{RF,l}^H \mathbf{g}_{l,1} e^{-j\phi}\right\} \tag{36}$$

$$= \arg \max_{\substack{\phi\in[-\pi,\pi) \\ \mathbf{f}_{RF,l}\in\frac{1}{\sqrt{N_t}}\{\pm 1\}^{N_t}}} \sum_{i=1}^{N_t} \mathbf{f}_{RF,l}(i)|\mathbf{g}_{l,1}(i)|\cos(\phi - \psi_i) \tag{37}$$

where ψ_i denotes the phase of $\mathbf{g}_{l,1}(i)$. Obviously, given any $\phi \in [-\pi, \pi)$, the corresponding binary precoder that maximizes (37) is

$$\mathbf{f}_{RF,l}(i) = \frac{1}{\sqrt{N_t}}\text{sign}\left(\cos\left(\phi - \psi_i\right)\right), i = 1, \ldots, N_t. \tag{38}$$

With the conditionally optimal $\mathbf{f}_{RF,l}$ for any given ϕ shown in (38), we will now show that we can always construct a set of N_t candidate binary precoders $\mathcal{F}_l \triangleq \{\mathbf{f}_{l,1}, \ldots, \mathbf{f}_{l,N_t}\}$ and guarantee $\mathbf{f}_{RF,l}^{\star} \in \mathcal{F}_l$. Then, the maximization in (34) can be carried out over a set of only N_t candidates without loss of performance.

We first define the angles $\widehat{\psi}_i$, $i = 1, \ldots, N_t$, as

$$\widehat{\psi}_i \triangleq \begin{cases} \psi_i - \pi, & \text{if } \psi_i \in \left[\frac{\pi}{2}, \frac{3\pi}{2}\right), \\ \psi_i, & \text{if } \psi_i \in \left[-\frac{\pi}{2}, \frac{\pi}{2}\right), \end{cases} \tag{39}$$

so that $\widehat{\psi}_i \in [-\frac{\pi}{2}, \frac{\pi}{2})$. Then, we map the angles $\widehat{\psi}_i$ to $\widetilde{\psi}_i$, $i = 1, \ldots, N_t$, which are rearranged in ascending order, i.e. $\widetilde{\psi}_1 \leq \widetilde{\psi}_2 \leq \ldots \leq \widetilde{\psi}_{N_t}$. Because of the periodicity of the cosine function, the maximization problem (37) with respect to ϕ can be carried out over any interval of length π. If we construct N_t non-overlapping sub-intervals $[\widetilde{\psi}_1 - \frac{\pi}{2}, \widetilde{\psi}_2 - \frac{\pi}{2}), [\widetilde{\psi}_2 - \frac{\pi}{2}, \widetilde{\psi}_3 - \frac{\pi}{2}), \ldots, [\widetilde{\psi}_{N_t} - \frac{\pi}{2}, \widetilde{\psi}_1 + \frac{\pi}{2})$, then the optimal $\phi^{\star}$ must be located in one of N_t sub-intervals since the full interval is $[\widetilde{\psi}_1 -$

$\frac{\pi}{2}, \widetilde{\psi}_1 + \frac{\pi}{2})$ of length π. Therefore, the optimization problem (37) can be solved by examining each sub-interval separately.

Assuming the optimal $\phi^\star$ is in the k-th sub-interval, the corresponding optimal binary precoder can be obtained by (38) as $\widetilde{\mathbf{f}}_{l,k}(i) = \frac{1}{\sqrt{N_t}}\text{sign}\left(\cos\left(\phi^\star - \widetilde{\psi}_i\right)\right)$, $i = 1, \ldots, N_t$, and has the form

$$\widetilde{\mathbf{f}}_{l,k} = \frac{1}{\sqrt{N_t}}[\underbrace{1 \ldots 1}_{k}\underbrace{-1 \ldots -1}_{N_t-k}]^T. \tag{40}$$

After that, given the inverse sorting that maps $\widetilde{\psi}_i$ to $\widehat{\psi}_i$, we rearrange the corresponding elements of $\widetilde{\mathbf{f}}_{l,k}$ and obtain $\widehat{\mathbf{f}}_{l,k}$. Then, based on the relationship between ψ_i and $\widehat{\psi}_i$ defined in (39), we can achieve the conditionally optimal precoder $\mathbf{f}_{l,k}$ by

$$\mathbf{f}_{l,k}(i) \triangleq \begin{cases} -\widehat{\mathbf{f}}_{l,k}(i), \text{ if } \psi_i \in \left[\frac{\pi}{2}, \frac{3\pi}{2}\right), i = 1, \ldots, N_t, \\ \widehat{\mathbf{f}}_{l,k}(i), \text{ if } \psi_i \in \left[-\frac{\pi}{2}, \frac{\pi}{2}\right), i = 1, \ldots, N_t, \end{cases} \tag{41}$$

for the case that $\phi^\star$ is in the k-th sub-interval.

Since the optimal $\phi^\star$ must be located in one of N_t sub-intervals, we can obtain N_t conditionally optimal precoders by examining all N_t sub-intervals and construct a candidate precoder set $\mathcal{F}_l$ as

$$\mathcal{F}_l \triangleq \{\mathbf{f}_{l,1}, \ldots, \mathbf{f}_{l,N_t}\}, \tag{42}$$

which must contain the optimal precoder $\mathbf{f}^\star_{RF,l}$. Therefore, without loss of performance, the problem in (34) can be transformed to an equivalent maximization task over only the set $\mathcal{F}_l$

$$\mathbf{f}^\star_{RF,l} = \arg \max_{\mathbf{f}_{RF,l} \in \mathcal{F}_l} \left|\mathbf{f}^H_{RF,l}\mathbf{g}_{l,1}\right|, \tag{43}$$

which has linear complexity $\mathcal{O}(N_t)$. Similarly, we can also construct a candidate analog combiner set $\mathcal{W}_l$ and obtain $\mathbf{w}^\star_{RF,l}$ by the same procedure.

The rank-1 solution returned by (43) is based on the rank-1 approximation of the interference-included equivalent channel $\mathbf{Q}_l$. The approximation of $\mathbf{Q}_l$ may cause a performance degradation when we revisit the original problem (30). Therefore, in order to enhance the performance, we propose to jointly select the precoder and combiner over candidate sets $\mathcal{F}_l$ and $\mathcal{W}_l$ as

$$\left\{\mathbf{f}^\star_{RF,l}, \mathbf{w}^\star_{RF,l}\right\} = \arg \max_{\substack{\mathbf{f}_{RF,l} \in \mathcal{F}_l \\ \mathbf{w}_{RF,l} \in \mathcal{W}_l}} \left|\mathbf{w}^H_{RF,l}\mathbf{Q}_l\mathbf{f}_{RF,l}\right| \tag{44}$$

which may return the rank-1 or a better solution with quadratic complexity $\mathcal{O}(N_tN_r)$. This low-complexity analog beamformer design with one-bit resolution PSs is summarized in Algorithm 2.

Algorithm 2 One-Bit Resolution Analog Beamformer Design

Input: $\mathbf{Q}_l$.
Output: $\mathbf{f}^\star_{RF,l}$ and $\mathbf{w}^\star_{RF,l}$.
1: Calculate $\mathbf{p}_{l,1}$ and $\mathbf{g}_{l,1}$ by an SVD of $\mathbf{Q}_l$.
2: Define the angles $\widehat{\psi}_i$, $i = 1, \ldots, N_t$, by (39).
3: Map $\widehat{\psi}_i$ to $\widetilde{\psi}_i$, $i = 1, \ldots, N_t$, in an ascending order.
4: **for** $k = 1 : N_t$ **do**
5: Obtain $\widetilde{\mathbf{f}}_{l,k}$ by (40).
6: Obtain $\widehat{\mathbf{f}}_{l,k}$ from $\widetilde{\mathbf{f}}_{l,k}$ based on inverse mapping from $\widetilde{\psi}_i$ to $\widehat{\psi}_i$, $i = 1, \ldots, N_t$.
7: Obtain $\mathbf{f}_{l,k}$ from $\widehat{\mathbf{f}}_{l,k}$ by (41).
8: **end for**
9: Construct $\mathcal{F}_l = \{\mathbf{f}_{l,1}, \ldots, \mathbf{f}_{l,N_t}\}$.
10: Construct $\mathcal{W}_l$ by a similar procedure as Steps 2-9.
11: Find the optimal $\mathbf{f}^\star_{RF,l}$ and $\mathbf{w}^\star_{RF,l}$ by (44).

V. Hybrid Precoder and Combiner Design for Multiuser mmWave MIMO Systems

In this section, we consider a mmWave multiuser MIMO uplink system and extend the low-resolution hybrid precoder and combiner designs proposed in the previous sections to the multiuser system.

A. System Model and Problem Formulation

We consider a multiuser mmWave MIMO uplink system as presented in Fig. 2, where a base-station (BS) is equipped with N_r antennas and N_{RF} RF chains and simultaneously serves K mobile users. Due to power consumption and hardware limitations, each mobile user has N_t antennas and a single RF chain to transmit only one data stream to the BS. We further assume the number of RF chains at the BS is equal to the number of users, i.e. $N_{RF} = K$.

Let $\mathbf{f}_{RF,k}$ be the analog precoder of the k-th user, where each element of $\mathbf{f}_{RF,k}$ has a constant magnitude $\frac{1}{\sqrt{N_t}}$ and low-resolution discrete phases, i.e. $\mathbf{f}_{RF,k}(i) \in \mathcal{F}$, $\forall i = 1, \ldots, N_t$. The transmitted signal of the k-th user after precoding can be formulated as

$$\mathbf{x}_k = \sqrt{P_k}\mathbf{f}_{RF,k}s_k \tag{45}$$

where s_k is the symbol of the k-th user, $\mathbb{E}\{|s_k|^2\} = 1$, and P_k is the k-th user's transmit power.

Let $\mathbf{H}_k \in \mathbb{C}^{N_r \times N_t}$, $k = 1, \ldots, K$, denote the uplink channel from the k-th user to the BS. The received signal at the BS can be written as

$$\mathbf{r} = \sum_{k=1}^{K} \sqrt{P_k}\mathbf{H}_k\mathbf{f}_{RF,k}s_k + \mathbf{n} \tag{46}$$

where $\mathbf{n} \sim \mathcal{CN}(\mathbf{0}, \sigma^2\mathbf{I}_{N_r})$ is complex Gaussian noise. The BS first applies an $N_r \times K$ analog combining matrix $\mathbf{W}_{RF} \triangleq [\mathbf{w}_{RF,1} \ldots \mathbf{w}_{RF,K}]$ to process the received signal, in which the analog combiner $\mathbf{w}_{RF,k}$ corresponding to the k-th user is also implemented by low-resolution PSs, i.e. $\mathbf{w}_{RF,k}(j) \in \mathcal{W}$, $j = 1, \ldots, N_r$. Then, a baseband digital combiner $\mathbf{w}_{BB,k} \in \mathbb{C}^{K \times 1}$ is employed to retrieve the information of the k-th user. Let $\mathbf{w}_k \triangleq \mathbf{W}_{RF}\mathbf{w}_{BB,k}$ denote the hybrid combiner corresponding to the k-th user. After the combining process at the BS, the estimated symbol of the k-th user can be expressed as

$$\hat{s}_k = \sqrt{P_k}\mathbf{w}_k^H\mathbf{H}_k\mathbf{f}_{RF,k}s_k + \mathbf{w}_k^H\sum_{\substack{i=1 \\ i \neq k}}^{K} \sqrt{P_i}\mathbf{H}_i\mathbf{f}_{RF,i}s_i + \mathbf{w}_k^H\mathbf{n}. \tag{47}$$

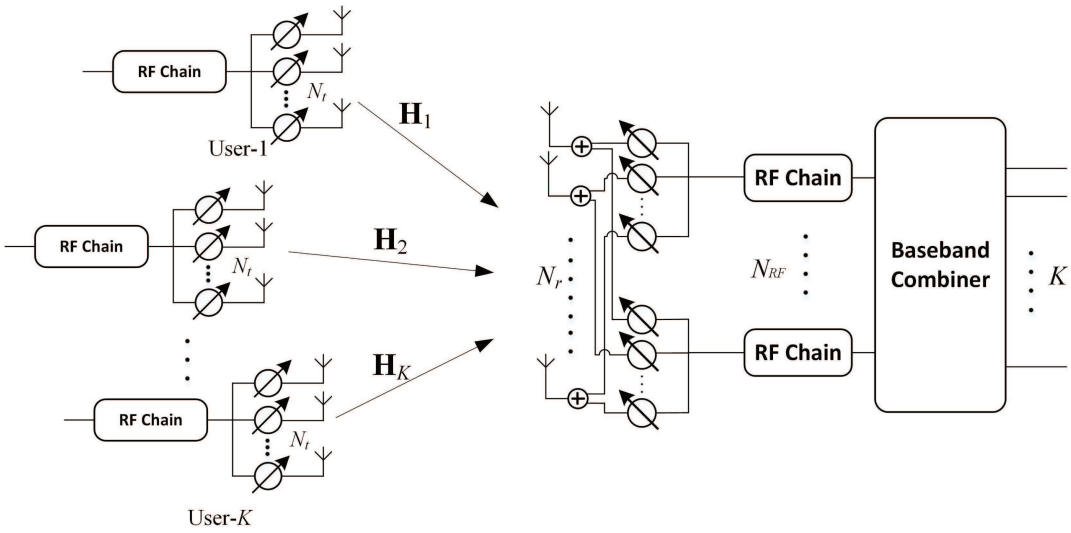


Fig. 2. The multiuser mmWave MIMO system using hybrid precoder and combiner.

Given the received signal at the BS in (47), the signal-to-interference-plus-noise ratio (SINR) of the k-th user can be expressed as

$$\gamma_k = \frac{\mid \sqrt{P_k}\mathbf{w}_k^H \mathbf{H}_k \mathbf{f}_{RF,k} \mid^2}{\sum\limits_{i=1,i\neq k}^{K} \mid \sqrt{P_i}\mathbf{w}_k^H \mathbf{H}_i \mathbf{f}_{RF,i} \mid^2 + \sigma^2 \parallel \mathbf{w}_k \parallel^2} \tag{48}$$

and the achievable sum-rate of the multiuser uplink system is

$$R_u = \sum_{k=1}^{K} \log(1+\gamma_k). \tag{49}$$

We aim to jointly design the analog precoders and combiners implemented by low-resolution PSs as well as the digital combiners to maximize the sum-rate of the uplink multiuser system:

$$\begin{aligned} \left\{ \left\{ \mathbf{w}_{RF,k}^{\star}, \mathbf{w}_{BB,k}^{\star}, \mathbf{f}_{RF,k}^{\star} \right\}_{k=1}^{K} \right\} = \arg\max \sum_{k=1}^{K} \log\left(1+\gamma_k\right) \\ \text{s. t.} \quad \mathbf{f}_{RF,k}(i) \in \mathcal{F},\ \forall k, i, \\ \mathbf{w}_{RF,k}(j) \in \mathcal{W},\ \forall k, j. \end{aligned} \tag{50}$$

B. Low-Resolution Hybrid Precoder and Combiner Design

Obviously, the optimization problem (50) cannot be directly solved. Thus, we adopt an approach similar to [26] and propose to successively design the low-resolution analog beamformer pair for each user, aiming at enhancing the channel gain as well as suppressing the inter-user interference. Then, the baseband combiner at the BS is calculated to further mitigate the interference and maximize the sum-rate.

In particular, for the first user, the analog precoder and combiner pair is designed to maximize the corresponding channel gain, which can be formulated as follows:

$$\begin{aligned} \left\{ \mathbf{w}_{RF,1}^{\star}, \mathbf{f}_{RF,1}^{\star} \right\} = \arg\max \left| \mathbf{w}_{RF,1}^H \mathbf{H}_1 \mathbf{f}_{RF,1} \right| \\ \text{s. t.} \quad \mathbf{f}_{RF,1}(i) \in \mathcal{F},\ i = 1, \ldots, N_t, \\ \mathbf{w}_{RF,1}(j) \in \mathcal{W},\ j = 1, \ldots, N_r. \end{aligned} \tag{51}$$

This analog precoder and combiner design problem can be efficiently solved by the algorithm presented in Sec. III-A when low-resolution PSs are utilized, or the algorithm proposed in Sec. IV if only one-bit resolution PSs are available. Then, the analog precoders $\mathbf{f}_{RF,k}$ and combiners $\mathbf{w}_{RF,k}$, $k = 2, 3, \ldots, K$, for the remaining $K-1$ users are successively designed by an iterative procedure. In each iteration, we attempt to find the analog beamformer pair that suppresses the interference from the users whose analog beamformers have already been determined. To achieve this goal, the channel of the user whose combiner is to be calculated is projected onto the space orthogonal to the collection of previously designed analog combiners. This approach leads to orthogonal analog combiners that suppress the inter-user interference.

Specifically, to design the k-th user's analog beamformer pair, we first extract the orthonormal components $\mathbf{d}_i$ of the previously determined analog combiners $\mathbf{w}_{RF,i}^{\star}$, $i = 1, \ldots, k-1$ by the Gram-Schmidt procedure:

$$\mathbf{q}_i = \mathbf{w}_{RF,i}^{\star} - \sum_{j=1}^{i-1} \mathbf{d}_j^H \mathbf{w}_{RF,i}^{\star} \mathbf{d}_j, \tag{52}$$

$$\mathbf{d}_i = \mathbf{q}_i / \|\mathbf{q}_i\|. \tag{53}$$

Note that $\mathbf{d}_1 = \mathbf{w}_{RF,1}^{\star}$ and $\mathbf{w}_{RF,1}^{\star}$ is the analog combiner calculated for the first user. Then, the combiner components are removed from the k-th user's channel to obtain the modified channel $\widehat{\mathbf{H}}_k$ as

$$\widehat{\mathbf{H}}_k = \left(\mathbf{I}_{N_r} - \sum_{i=1}^{k-1} \mathbf{d}_i \mathbf{d}_i^H \right) \mathbf{H}_k. \tag{54}$$

Finally, based on the modified channel $\widehat{\mathbf{H}}_k$, the analog beamformer pair for the k-th user is found by solving the following optimization using the algorithms proposed in the previous

sections:

$$\left\{\mathbf{w}_{RF,k}^{\star}, \mathbf{f}_{RF,k}^{\star}\right\} = \arg\max \left|\mathbf{w}_{RF,k}^{H} \widehat{\mathbf{H}}_k \mathbf{f}_{RF,k}\right| \quad \text{s. t.} \quad \mathbf{f}_{RF,k}(i) \in \mathcal{F},\ i = 1, \ldots, N_t, \quad \mathbf{w}_{RF,k}(j) \in \mathcal{W},\ j = 1, \ldots, N_r. \tag{55}$$

After finding the analog beamformers for all users, the effective baseband channel for each user can be obtained as $\mathbf{h}_k^e \triangleq \sqrt{P_k}\left(\mathbf{W}_{RF}^{\star}\right)^H \mathbf{H}_k \mathbf{f}_{RF,k}^{\star}$. Then, a minimum mean square error (MMSE) baseband digital combiner for the k-th user is employed to further suppress the interference:

$$\mathbf{w}_{BB,k}^{\star} = \left[\mathbf{H}^e (\mathbf{H}^e)^H + \sigma^2 \left(\mathbf{W}_{RF}^{\star}\right)^H \mathbf{W}_{RF}^{\star}\right]^{-1} \mathbf{h}_k^e, \tag{56}$$

where $\mathbf{H}^e \triangleq [\mathbf{h}_1^e, \ldots, \mathbf{h}_K^e]$. The proposed low-resolution hybrid precoder and combiner design for multiuser mmWave systems is summarized in Algorithm 3.

Algorithm 3 Low-Resolution Hybrid Precoder and Combiner Design for Multiuser mmWave Systems

Input: $\mathcal{F}$, $\mathcal{W}$, $\mathbf{H}_k$, $k = 1, \ldots, K$.

Output: $\mathbf{f}_{RF,k}^{\star}$, $\mathbf{w}_{RF,k}^{\star}$, $\mathbf{w}_{BB,k}^{\star}$, $k = 1, \ldots, K$.

1: Obtain $\mathbf{w}_{RF,1}^{\star}$ and $\mathbf{f}_{RF,1}^{\star}$ for user-1 by solving

$$\left\{\mathbf{w}_{RF,1}^{\star}, \mathbf{f}_{RF,1}^{\star}\right\} = \arg \max_{\substack{\mathbf{w}_{RF,1}(i) \in \mathcal{W} \\ \mathbf{f}_{RF,1}(j) \in \mathcal{F}}} |\mathbf{w}_{RF,1}^H \mathbf{H}_1 \mathbf{f}_{RF,1}|.$$

2: $\mathbf{d}_1 = \mathbf{w}_{RF,1}^{\star}$.

3: **for** $k = 2 : K$ **do**

4: $\quad \widehat{\mathbf{H}}_k = \left(\mathbf{I}_{N_r} - \sum_{i=1}^{k-1} \mathbf{d}_i \mathbf{d}_i^H\right) \mathbf{H}_k$.

5: $\quad$ Obtain $\mathbf{w}_{RF,k}^{\star}$ and $\mathbf{f}_{RF,k}^{\star}$ for user-k by solving

$$\left\{\mathbf{w}_{RF,k}^{\star}, \mathbf{f}_{RF,k}^{\star}\right\} = \arg \max_{\substack{\mathbf{w}_{RF,k}(i) \in \mathcal{W} \\ \mathbf{f}_{RF,k}(j) \in \mathcal{F}}} |\mathbf{w}_{RF,k}^H \widehat{\mathbf{H}}_k \mathbf{f}_{RF,k}|.$$

6: $\quad \mathbf{q}_k = \mathbf{w}_{RF,k}^{\star} - \sum_{i=1}^{k-1} \mathbf{d}_i^H \mathbf{w}_{RF,k}^{\star} \mathbf{d}_i$;

7: $\quad \mathbf{d}_k = \mathbf{q}_k / \|\mathbf{q}_k\|$.

8: **end for**

9: Obtain digital combiners $\mathbf{w}_{BB,k}^{\star}$, $k = 1, \ldots, K$, by

$$\mathbf{w}_{BB,k}^{\star} = \left[\mathbf{H}^e (\mathbf{H}^e)^H + \sigma^2 \left(\mathbf{W}_{RF}^{\star}\right)^H \mathbf{W}_{RF}^{\star}\right]^{-1} \mathbf{h}_k^e.$$

VI. Simulation Results

In this section, we provide simulation results for the proposed joint hybrid precoder and combiner designs with low-resolution PSs for point-to-point mmWave systems as well as multiuser mmWave systems. MmWave channels are expected to be sparse and have a limited number of propagation paths. In the simulations, we adopt a geometric channel model with L paths [32]. In particular, the discrete-time narrow-band mmWave channel $\mathbf{H}$ is formulated as

$$\mathbf{H} = \sqrt{\frac{N_t N_r}{L}} \sum_{i=1}^{L} \alpha_i \mathbf{a}_r(\theta_i^r) \mathbf{a}_t(\theta_i^t)^H \tag{57}$$

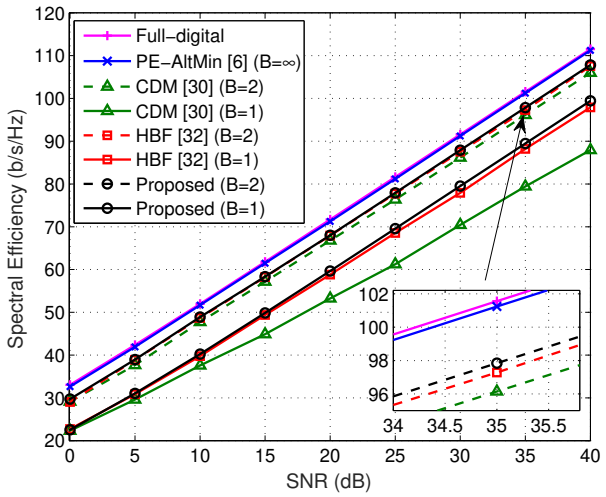


Fig. 3. Spectral efficiency versus SNR ($N_t = 64$, $N_r = 64$, $N_t^{RF} = N_r^{RF} = 6$, $N_s = 6$).

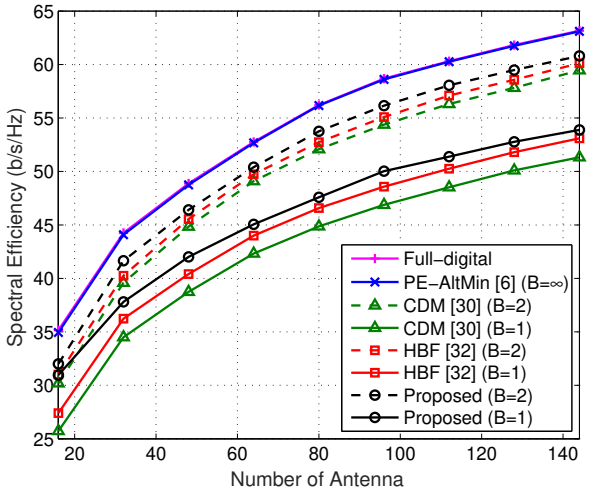


Fig. 4. Spectral efficiency versus number of antenna ($N_t^{RF} = N_r^{RF} = 4$, $N_s = 4$, SNR = 20dB).

where $\alpha_i \sim \mathcal{CN}(0, \frac{1}{L})$ are the independent and identically distributed complex gains of the i-th propagation path (ray) θ_i^t and $\theta_i^r \in [-\frac{\pi}{2}, \frac{\pi}{2}]$ are the angles of departure (AoD) and the angles of arrival (AoA), respectively. Finally, the array response vectors $\mathbf{a}_t(\theta^t)$ and $\mathbf{a}_r(\theta^r)$ depend on the antenna array geometry. We assume that the commonly used uniform linear arrays (ULAs) are employed, and the transmit antenna array response vector $\mathbf{a}_t(\theta^t)$ and the receive antenna array response vector $\mathbf{a}_r(\theta^r)$ can be written as

$$\mathbf{a}_t(\theta^t) = \frac{1}{\sqrt{N_t}}[1, e^{j\frac{2\pi}{\lambda} d \sin(\theta^t)}, \ldots, e^{j(N_t-1)\frac{2\pi}{\lambda} d \sin(\theta^t)}]^T, \tag{58}$$

$$\mathbf{a}_r(\theta^r) = \frac{1}{\sqrt{N_r}}[1, e^{j\frac{2\pi}{\lambda} d \sin(\theta^r)}, \ldots, e^{j(N_r-1)\frac{2\pi}{\lambda} d \sin(\theta^r)}]^T, \tag{59}$$

respectively, where λ is the signal wavelength, and d is the distance between antenna elements. In the following simulations, we consider an environment with $L = 6$ scatterers between the

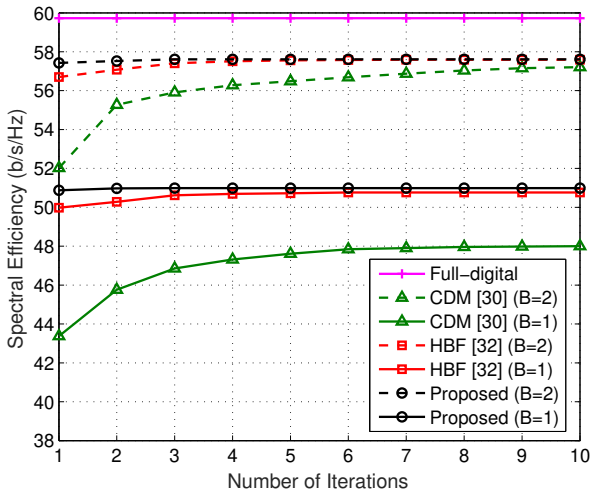


Fig. 5. Spectral efficiency versus number of iteration ($N_t = 64, N_r = 64$, $N_t^{RF} = N_r^{RF} = 4$, $N_s = 4$, SNR = 20dB).

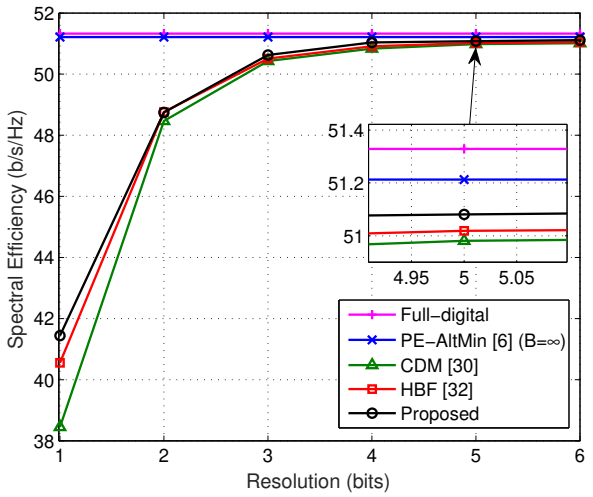


Fig. 6. Spectral efficiency versus resolution of PSs ($N_t = 64$, $N_r = 64$, $N_t^{RF} = N_r^{RF} = 4$, $N_s = 4$, SNR = 20dB).

transmitter and the receiver. The antenna spacing is $d = \frac{\lambda}{2}$.

A. Simulation Results of a Point-to-Point mmWave System

We first consider a point-to-point mmWave communication system, in which the transmitter and receiver are both equipped with 64-antenna ULAs. The number of RF chains at the transmitter and receiver are $N_t^{RF} = N_r^{RF} = 6$, so the number of data streams is also assumed to be $N_s = 6$.

Fig. 3 shows the average spectral efficiency versus SNR over 10^6 channel realizations. We evaluate the spectral efficiency of the algorithm proposed in Sec. III for the case of 2-bit ($B = 2$) resolution PSs and the algorithm proposed in Sec. IV for the case of 1-bit ($B = 1$) resolution PSs. For comparison purposes, we also plot the spectral efficiency of two state-of-the-art low-resolution hybrid beamformer designs: the coordinate descent method (CDM) algorithm in [30] and the hybrid beamforming (HBF) algorithm in [32]. To the best of our knowledge, the algorithm in [32] achieves the best performance with low-resolution PSs in the existing literature. The performance of a fully digital approach using SVD-based beamforming and the hybrid beamforming scheme with infinite-resolution ($B = \infty$) PSs using the phase extraction (PE-AltMin) algorithm in [6] are also included as performance benchmarks. Fig. 3 illustrates that the proposed algorithm outperforms the competitors, particularly for the case of 1-bit resolution PSs. Moreover, it can be observed that the proposed algorithm with $B = 2$ achieves performance close to optimal full-digital beamforming and hybrid beamforming with infinite-resolution PSs. For additional simulation validation, Fig. 4 illustrates the spectral efficiency versus the number of antennas and similar conclusions can be drawn.

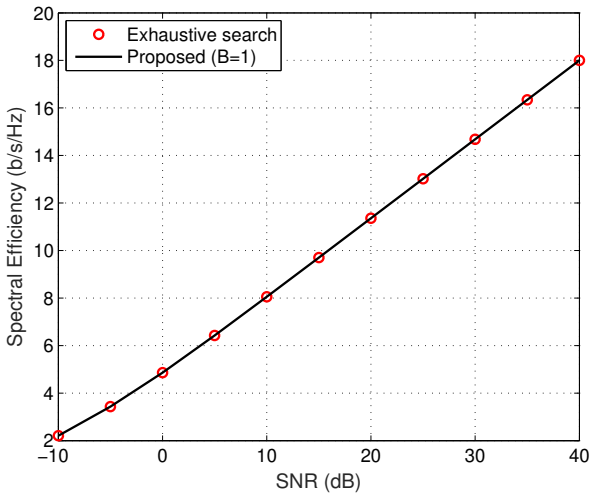


Fig. 7. Spectral efficiency versus SNR ($N_t = 8$, $N_r = 8$, $N_s = 1$, $B = 1$).

In order to illustrate the convergence of the proposed algorithm, we show the spectral efficiency versus the number of iterations in Fig. 5, which also includes other algorithms for comparison. It is observed that our proposed algorithms converge faster than the other two iterative schemes, which is a highly favorable property. In Fig. 6, we show the spectral efficiency as a function of B to illustrate the impact of the resolution of PSs on the spectral efficiency. As expected, increasing the PS resolution will improve the system performance, but using only $B = 3$ bits is sufficient to closely approach the performance of the ideal unquantized case. Beyond $B = 3$, the additional cost and complexity associated with using higher-resolution PSs is not warranted given the very marginal increase in spectral efficiency. Moreover, our proposed algorithms outperform the other two low-resolution beamforming methods for all PS resolutions.

To examine the impact of the approximations used in deriving the proposed one-bit resolution hybrid beamformer scheme, in Fig. 7 we compare it with the optimal exhaustive search approach. The number of antennas at both transmitter and receiver is chosen to be 8 and the number of data streams is $N_s = 1$. A relatively simple case is examined here due to the exponential complexity of the exhaustive search method. We see from Fig. 7 that the spectral efficiency achieved by

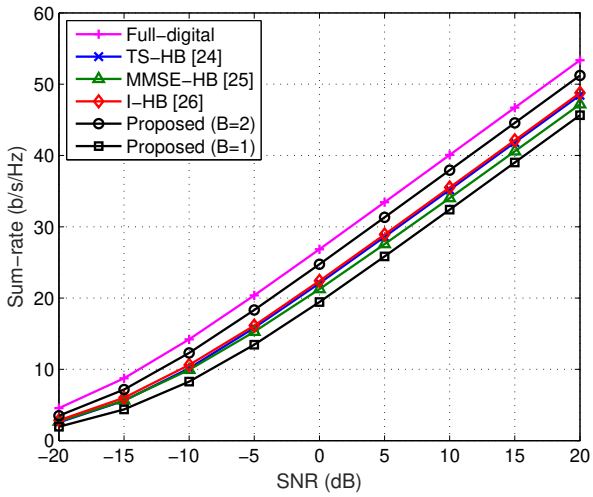


Fig. 8. Spectral efficiency versus SNR ($N_t = 64$, $N_r = 16$, $N_t^{RF} = 4$, $K = 4$).

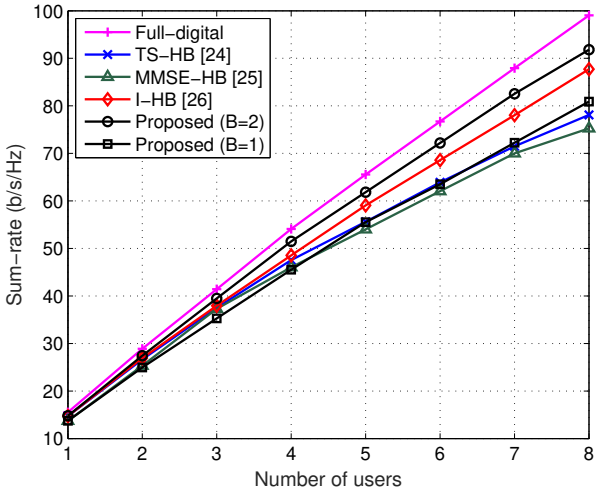


Fig. 9. Spectral efficiency versus K ($N_t = 64, N_r = 16$, $N_t^{RF} = K$, SNR = 20dB).

the proposed algorithm is the same as that of the optimal exhaustive search method, suggesting that the proposed hybrid beamforming algorithm with one-bit resolution PSs can provide optimal or near-optimal performance.

B. Simulation Results of a Multiuser mmWave System

Next, we evaluate the performance of the proposed low-resolution beamformer algorithm in a multiuser uplink system. We assume there are $K = 4$ users, each of which is equipped with $N_t = 16$ antennas and only one RF chain to transmit a single data stream. The BS has $N_r = 64$ antennas and $N_r^{RF} = 4$ RF chains. Fig. 8 illustrates the sum-rate versus SNR for various hybrid beamformer designs. In particular, we include three state-of-the-art multiuser hybrid beamforming approaches for comparison: *i*) two-stage hybrid beamforming (TS-HB) in [24], *ii*) MMSE-based hybrid beamforming (MMSE-HB) in [25], and *iii*) iterative hybrid beamforming (I-HB) in [26]. All three algorithms are codebook-based approaches and the size of the beamsteering codebook is set at 32 (i.e. $B = 5$ quantization bits) for fairness of the comparison. It can be observed from Fig. 8 that our proposed low-resolution hybrid beamforming design outperforms the other three algorithms using only 2-bit resolution PSs. Moreover, the performance with 1-bit resolution PSs is also comparable. Fig. 9 further shows the sum-rate versus the number of users K. From Fig. 9, we see that our proposed algorithm with 2-bit resolution PSs always outperforms the other codebook-based algorithms. Furthermore, even with 1-bit resolution PSs, the proposed algorithm can still achieve competitive performance compared with the TS-HB and MMSE-HB approaches when $K > 5$.

VII. Conclusions

This paper considered the problem of hybrid precoder and combiner design for mmWave MIMO systems with low-resolution quantized PSs. We proposed an efficient iterative algorithm which successively designs the low-resolution analog precoder and combiner pair for each data stream. Then, the digital precoder and combiner were computed based on the obtained effective baseband channel to further enhance the spectral efficiency. The design of low-resolution hybrid beamformers for multiuser MIMO communication systems was also investigated. Simulation results verified the effectiveness of the proposed algorithms, particularly for scenarios in which one-bit resolution phase shifters are used.

Appendix A
Proof of Proposition 1

The optimization problem (19) can be equivalently formulated as

$$\max \left| \frac{1}{\sqrt{N_t N_r}} \sum_{j=1}^{N_r} e^{j\varphi_j^l} \sum_{i=1}^{N_t} e^{j\vartheta_i^l} \mathbf{Q}_l(j,i) \right|. \tag{60}$$

By discarding the constant coefficient $1/\sqrt{N_t N_r}$, (60) can be further transformed as

$$\max \left| \sum_{j=1}^{N_r} e^{j\varphi_j^l} \left\{ e^{j\vartheta_i^l} \mathbf{Q}_l(j,i) + \sum_{u \neq i}^{N_t} e^{j\vartheta_u^l} \mathbf{Q}_l(j,u) \right\} \right|. \tag{61}$$

Since the term $e^{j\vartheta_i^l}$ does not involve the summation index j, it can be put outside the first summation, resulting in

$$\max \left| e^{j\vartheta_i^l} \sum_{j=1}^{N_r} e^{j\varphi_j^l} \mathbf{Q}_l(j,i) + \sum_{j=1}^{N_r} e^{j\varphi_j^l} \sum_{u \neq i}^{N_t} e^{j\vartheta_u^l} \mathbf{Q}_l(j,u) \right|. \tag{62}$$

Obviously, the optimal value of ϑ_i^l makes the phases of the first and second term equal to obtain the largest amplitude, and (20) is proved. ■

REFERENCES

[1] Z. Pi and F. Khan, "An introduction to millimeter-wave mobile broadband systems," *IEEE Commun. Mag.*, vol. 49, no. 6, pp. 101-107, June 2011.

[2] T. Rappaport, S. Sun, R. Mayzus, H. Zhao, Y. Azar, K. Wang, G. N. Wong, J. K. Schulz, M. Samimi, and F. Gutierrez "Millimeter wave mobile communications for 5G cellular: It will work!" *IEEE Access*, vol. 1, pp. 335-349, 2013.

[3] A. Lee Swindlehurst, E. Ayanoglu, P. Heydari, and F. Capolino, "Millimeter-wave massive MIMO: The next wireless revolution?" *IEEE Commun. Mag.*, vol. 52, no. 9, pp. 56-62, Sept. 2014.

[4] T. S. Rappapport, G. R. MacCartney, M. K. Samimi, and S. Sun, "Wideband millimeter-wave propagation measurements and channel models for future wireless communication system design", *IEEE Trans. Commun.*, vol. 63, no. 9, pp. 3029-3056, Sept. 2015.

[5] R. W. Heath Jr., N. González-Prelcic, S. Rangan, W. Roh, and A. M. Sayeed, "An overview of signal processing techniques for millimeter wave MIMO systems," *IEEE J. Sel. Topics Signal Process.*, vol. 10, no. 3, pp. 436-453, April 2016.

[6] X. Yu, J.-C. Shen, J. Zhang, and K. B. Letaief, "Alternating minimization algorithms for hybrid precoding in millimeter wave MIMO systems," *IEEE J. Sel. Topics Signal Process.*, vol. 10, no. 3, pp. 485-500, April 2016.

[7] C. Rusu, R. Méndez-Rial, N. González-Prelcic, and R. W. Heath Jr., "Low complexity hybrid precoding strategies for millimeter wave communication systems," *IEEE Trans. Wireless Commun.*, vol. 15, no. 12, pp. 8380-8393, Sept. 2016.

[8] R. López-Valcarce, N. González-Prelcic, C. Rusu, and R. W. Heath Jr., "Hybrid precoders and combiners for mmWave MIMO systems with per-antenna power constraints." in *Proc. IEEE Global Communication Conference (GLOBECOM)*, Washington, DC, Dec. 2016, pp. 1-6.

[9] C.-E. Chen, "An iterative hybrid transceiver design algorithm for millimeter wave MIMO systems," *IEEE Wireless Commun. Lett.*, vol. 4, no. 3, pp. 285-288, June 2015.

[10] W. Ni, X. Dong, and W.-S. Lu, "Near-optimal hybrid processing for massive MIMO systems via matrix decomposition," *IEEE Trans. Signal Process.*, vol. 65, no. 15, pp. 3922-3933, Aug. 2017.

[11] X. Gao, L. Dai, S. Han, C.-L. I, and R. W. Heath Jr., "Energy-efficient hybrid analog and digital precoding for mmWave MIMO systems with large antenna arrays," *IEEE J. Sel. Areas Commun.*, vol. 34, no. 4, pp. 998-1009, April 2016.

[12] L. Dai, X. Gao, J. Quan, S. Han, and C.-L. I, "Near-optimal hybrid analog and digital precoding for downlink mmWave massive MIMO systems", in *Proc. IEEE Int. Conf. Commun. (ICC)*, London, UK, June 2015, pp. 1334-1339.

[13] S. He, C. Qi, Y. Wu, and Y. Huang, "Energy-efficient transceiver design for hybrid sub-array architecture MIMO systems," *IEEE Access*, vol. 4, pp. 9895-9905, 2016.

[14] O. E. Ayach, S. Rajagopal, S. Abu-Surra, Z. Pi, and R. W. Heath Jr., "Spatially sparse precoding in millimeter wave MIMO systems," *IEEE Trans. Wireless Commun.*, vol. 13, no. 3, pp. 1499-1513, Mar. 2014.

[15] A. Alkhateeb, O. El Ayach, G. Leus, and R. W. Heath Jr., "Channel estimation and hybrid precoding for millimeter wave cellular systems," *IEEE J. Sel. Topics Signal Process.*, vol. 8, no. 5, pp. 831-846, Oct. 2014.

[16] C. Rusu, R. Méndez-Rial, N. González-Prelcic, and R. W. Heath Jr., "Low complexity hybrid sparse precoding and combining in millimeter wave MIMO systems," *IEEE Int. Conf. on Commun. (ICC)*, London, UK, June 2015, pp. 1340-1345.

[17] J.-C. Chen, "Efficient codebook-based beamforming algorithm for millimeter-wave massive MIMO systems," *IEEE Trans. Veh. Technol.*, to Appear.

[18] X. Gao, L. Dai, C. Yuen, and Z. Wang, "Turbo-like beamforming based on Tabu search algorithm for millimeter-wave massive MIMO systems," *IEEE Trans. Veh. Technol.*, vol. 65, no. 7, pp. 5731-5737, July 2016.

[19] S. Han, C.-L. I, Z. Xu, and C. Rowell, "Large-scale antenna systems with hybrid analog and digital beamforming for millimeter wave 5G," *IEEE Commun. Mag.*, vol. 53, no. 1, pp. 186-194, Jan. 2015.

[20] A. Li and C. Masouros, "Hybrid analog-digital millimeter-wave MU-MIMO transmission with virtual path selection," *IEEE Commun. Lett.*, vol. 21, no. 2, pp. 438-441, Feb. 2017.

[21] L. Liang, W. Xu, and X. Dong, "Low-complexity hybrid precoding in massive multiuser MIMO systems," *IEEE Wireless Commun. Lett.*, vol. 3, no. 6, pp. 653-656, Dec. 2014.

[22] A. Li and C. Masouros, "Hybrid precoding and combining design for millimeter-wave multi-user MIMO based on SVD," *IEEE Int. Conf. on Commun. (ICC)*, Paris, France, May 2017, pp. 1-6.

[23] M. Kim and Y. H. Lee, "MSE-based hybrid RF/baseband processing for millimeter-wave communication systems in MIMO interference channels," *IEEE Trans. Veh. Technol.*, vol. 64, no. 6, pp. 2714-2720, June 2015.

[24] A. Alkhateeb, G. Leus, and R. W. Heath Jr., "Limited feedback hybrid precoding for multi-user millimeter wave systems," *IEEE Trans. Wireless Commun.*, vol. 14, no. 11, pp. 6481-6494, Nov. 2015.

[25] D. H. N. Nguyen, L. B. Le, and T. Le-Ngoc, "Hybrid MMSE precoding for mmWave multiuser MIMO systems," *IEEE Int. Conf. on Commun. (ICC)*, Kuala Lumpur, Malaysia, May 2016.

[26] Z. Wang, M. Li, X. Tian, and Q. Liu, "Iterative hybrid precoder and combiner design for mmWave multiuser MIMO systems," *IEEE Commun. Lett.*, vol. 21, no. 7, pp. 1581-1584, July 2017.

[27] T. E. Bogale, L. B. Le, A. Haghighat, and L. Vandendorpe, "On the number of RF chains and phase shifters, and scheduling design with hybrid analog-digital beamforming," *IEEE Trans. Wireless Commun.*, vol. 15, no. 5, pp. 3311-3326, May 2016.

[28] A. S. Y. Poon and M. Taghivand, "Supporting and enabling circuits for antenna arrays in wireless communications," *Proc. IEEE*, vol. 100, no. 7, pp. 2207-2218, July 2012.

[29] R. Méndez-Rial, C. Rusu, N. González-Prelcic, and A. Alkhateeb, "Hybrid MIMO architectures for millimeter wave communications: Phase shifters or switches?", *IEEE Access*, vol. 4, pp. 247-267, March 2016.

[30] J.-C. Chen, "Hyrbrid beamforming with discrete phase shifters for millimeter-wave massive MIMO systems," *IEEE Trans. Veh. Technol.*, to Appear.

[31] F. Sohrabi and W. Yu, "Hybrid beamforming with finite-resolution phase shifters for large-scale MIMO systems," in *Proc. IEEE Workshop Signal Process. Adv. Wireless Commun. (SPAWC)*, Stockholm, Sweden, June 2015, pp. 136-140.

[32] F. Sohrabi and W. Yu, "Hybrid digital and analog beamforming design for large-scale antenna arrays," *IEEE J. Sel. Topics Signal Process.*, vol. 10, no. 3, pp. 501-513, April 2016.

[33] G. N. Karystinos and D. A. Pados, "Rank-2-optimal adaptive design of binary spreading codes," *IEEE Trans. Inf. Theory*, vol. 53, no. 9, pp. 3075-3080, Sept. 2007.

[34] G. H. Golub and C. F. Van Loan, *Matrix Computations*. Baltimore, USA: JHU Press, 2012.